

General Sensorless Method with Parameter Identification and Double Kalman Filter Applied to a Bistable Fast Linear Switched Reluctance Actuator for Textile Machine

Douglas Martins Araujo^{*a)} Non-member, Faguy Tamwo Simo^{*} Non-member
Yves Perriard^{*} Non-member

(Manuscript received Oct. 26, 2017, revised Sep. 18, 2018)

This paper provides a general sensorless method to control the position of a linear actuator. After a review of the solutions used so far, this new method is applied to identify keys passing through a linear actuator used in an industrial textile machine. The presented method describes how to find out the position of the key using two cascading discrete Kalman filters, the first for filtering the speed and the second for filtering the impedance measurement in order to retrieve the position. To speed-up the method and due to the thickness difference from one textile machine to another, an actuator model, to evaluate impedance in function of the position, is obtained by using parameter identification. Kalman's filter parameters are optimized to minimize the time necessary to learn the speed operation. Finally, we focus on the temporal evolution of Kalman Filters parameters on the learning process.

Keywords: actuator, experimental validation, Kalman filter, linear switched reluctance, position control, sensorless

1. Introduction

Linear motors, whose strength has electromagnetic origin, can be classified as (1): Linear induction motor; Linear synchronous motor; DC brushless motor; DC motor with brushes.

In general, the linear actuator has some advantages compared to the use of rotating motors, such as the elimination of the mechanical elements required to transform rotational motion into translational motion and consequent increase in mechanical efficiency (2). Among the main applications are production systems such as machine tools (4), or high-speed trains.

In this paper, we focus on one type of DC brushless motor: the Linear Switched Reluctance Motor (LSRM). Some of these motors can present magnets on the fixed part, the mobile part remaining free of magnets and the strength continues to be produced by reluctances forces. This last can be classified as Hybrid Linear Switched Reluctance Motor and this is the kind of device that we aim to study. Thanks to the magnet, even when the coil are not active a reluctance force appears and in case of movement, the voltage of the coil can be perturbed. Then, to drive these motors, controlling the position or speed without sensor, these characteristics have to be taking into account.

1.1 Sensorless Techniques Many sensorless solutions to find the position have been studied. The most successful are high frequency signal injection (3) and impedance

variation (4). Both methods are used to control several types of motors.

The signal injection technique consist to find an adapted frequency in which the answer of the system allows to observe, for example, the position of the motor. For a given frequency, the perturbation on an internal electric state variable reproduces the evolution of another mechanical state variable. Besides the cost of it implementation, this method has one important drawback: it cannot be used if the perturbation on the electric state variable, produced by the signal injection, is big enough to ruin the motor control.

If Hybrid Linear Switched Reluctance Motor, what we aim to study, is very sensitive to these perturbations, due to the presence of a magnet, then other techniques have to be employed.

The impedance variation method consists in associating this variation to the mechanical state variable (for example, the position). General speaking, this variation can have two origins: modification of the total equivalent reluctance due to movements or presence of Eddy currents. The effects of Eddy currents are in general minimized by introducing laminated material on the iron parts. Finally, the variation due to geometry reconfiguration seems to be the better option in our case.

In order to drive the motor, by using sensorless technique, the impedance must be measured in real time, which can be an expensive procedure. To avoid using expensive drives, the real position of the actuator is obtained by using one or more Kalman filters, as used in (5).

2. Problem Chosen as an Example

Industrial textile machines use Hybrid Linear Switched Reluctance Actuator to drive keys in and out to achieve

a) Correspondence to: Douglas Martins Araujo. E-mail: douglas.martins.araujo@cern.ch

^{*} Ecole Polytechnique Fédérale de Lausanne (EPFL) Integrated Actuators Laboratory (LAI)
CH-2002 Neuchâtel, Switzerland

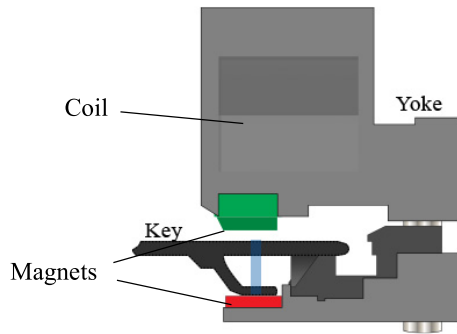


Fig. 1. Textile machine actuator

knitting purpose. In such machines, magnetic sensors are used for detecting and counting the keys. Thus, the overall process of knitting relies on those sensors which is a critical point of reliability because one failure makes the knitting purpose impossible.

We aim to improve the reliability of a textile machine by developing a new sensorless solution for detecting and counting the keys, which means controlling the position. The studied device has one stator (the bulk of the actuator) and one moving part (the keys) the configuration of the magnetic circuit changes periodically with the position. This variation in the magnetic circuit modifies the level of impedance and we can use impedance measurements, as explained before, for our sensorless position control. However, in practical applications, the impedance is obtained by measuring voltage and current which are contaminated by various noises. Thus, the measurements need to be filtered and for this reason we have first to develop an analytical model giving the level of impedance with respect to the position of the actuator and then a discrete Kalman filter for filtering impedance measurement has been developed (6) and (7).

Figure 1 illustrates the actuator, with its magnet and yoke, and the mobile key.

Due to thickness differences from one textile machine to another, an actuator model, to evaluate impedance in function of the position, is obtained by using parameter identification. According to (8), generally this kind of actuator has a very complex geometry and the identification parameter method is a way to avoid building a model to these actuators. Furthermore, the keys are different from each other. Some are more used than others or some are more lubricated than others. Due to the collision with the actuator, some keys are deformed with the time of use. Consequently, the disturbance in terms of impedance, due to each key is different. A Kalman filter can be used to identify the passage of the keys despite the difference between them.

The textile process can be achieved by using different speeds. This speed referees to the mobile part fed by the actuator which we are studding. Then the impedance profile changes in function of the speed. This is why a Kalman filter should be used in order to identify the speed.

Figure 2 shows a textile machine with the mobile wagon fed by actuators. Depending on the actuators, keys can be selected in one direction or another. Unlike the standard actuators, the passive part (keys) is fixed and the active part moves with the wagon.

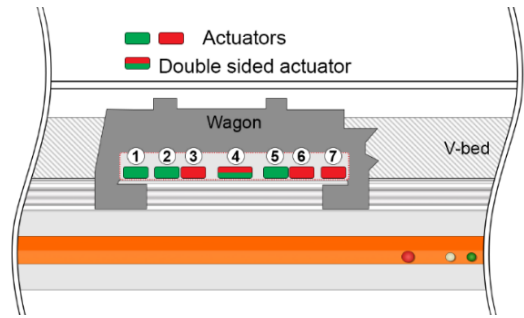


Fig. 2. Textile machine with its wagon and V-bed

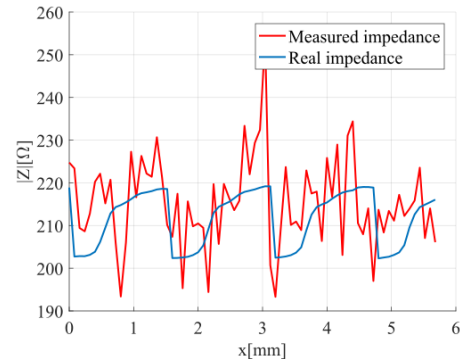


Fig. 3. Comparison between U-I measured data and impedance meter data

This paper presents a sensorless solution using two cascading Kalman filters, the first calculating the speed of the wagon and the second for filtering the noisy impedance measurements to retrieve the position and thus drive the keys.

To summarize, our application can be compared to a switched reluctance linear drive with several specificities. Equivalent circuits of these drives are well known which allows to establish a very strong correlation between electrical and mechanical variables. In our case, this correlation isn't established on literature and since our drive can be crossed by different keys, it becomes very difficult to define these relations. This situation is equivalent to a drive in which the mobile part can be changed dynamically. To solve this issue, we propose to use a model optimized using measurement. By doing this, when the keys are changed a simple and automated measurement can update the model. Counter to standard motors, each key can response differently in respect to speed. Due to aging phenomena, the impedance in function of position from one key to another is very different, special when the speed varies. This is way, for our application, two Kalman filters are used: one to estimate the speed and the second one to the position.

3. General Idea of the Proposed Method

Our sensorless method is mainly based on the impedance measurements, the method implemented for this purpose is to inject a sinusoidal voltage and the resulting current is then measured for the determination of the impedance value. For a given wagon's speed, Figure 3 shows the impedance in function of the position:

- the impedance measured using Voltage-Current both acquired from an oscilloscope (in red);
- the impedance measured by a high resolution impedance

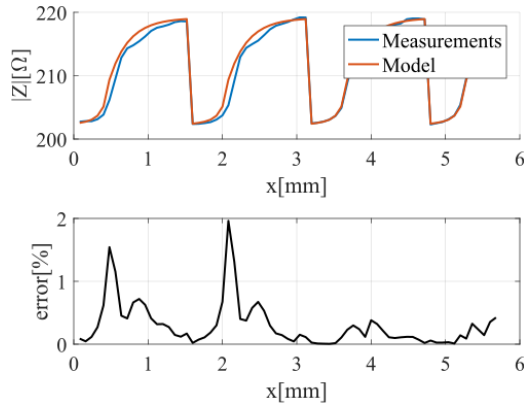


Fig. 4. Comparison between the model and the measured data

meter Agilent 4294A where the auto balancing bridge method is implemented (9) (in blue).

It is obvious that the measured impedance, is very unstable and unusable to correctly detect the key presence in the actuator (pics in the impedance curve). Consequently, impedance measurements have to be filtered, in this case the Kalman filter algorithm can be very effective. Therefore, a good model of the actuator is needed in order to produce a reference impedance to the filtering process.

4. Actuator Model

Deriving an actuator model based on the interpretation of physical phenomenon (10) was difficult to achieve for the following reasons:

- the bulk has a non-regular geometry and it is composed of assembled elements of different natures and its physical characteristics are not a priori known,
- the keys have different thicknesses from one textile machine to another.

We propose a new analytical model giving the level of impedance with respect to the position. The position is denoted as x and it variates from a given position to the P_c , where P_c is the total distance between two consecutives keys. The model is defined as follows:

$$|Z|(x) = \begin{cases} a_1 e^{b_1 x} + a_2 e^{b_2 x} & x \in \left[0, \frac{e}{2}\right] \\ a_3 + a_4 \left(1 - e^{b_3 \left(\frac{e}{2} - x\right)}\right) & x \in \left[\frac{e}{2}, P_c\right], \end{cases} \quad \dots \quad (1)$$

where $a_1, a_2, a_3, a_4, b_1, b_2, b_3$ are the model parameters and e the key thickness in millimeter. The proposed model is obtained in two steps: at first using the MATLAB fitting curve toolbox, we have performed data analysis, for defining a parametric fitting function. Secondly using measured data, and after solving an inverse problem of optimisation by genetic algorithm, with error minimisation as objective function, the optimum values of theses parameters are found out. Figure 4 shows the comparison between the model and the measured data, and also the error between the model and the measured data with respect to the position.

The impedance shown in Fig. 4 has been obtained a priori by moving the wagon manually. By doing this we can ensure no influence of speed when performing impedance

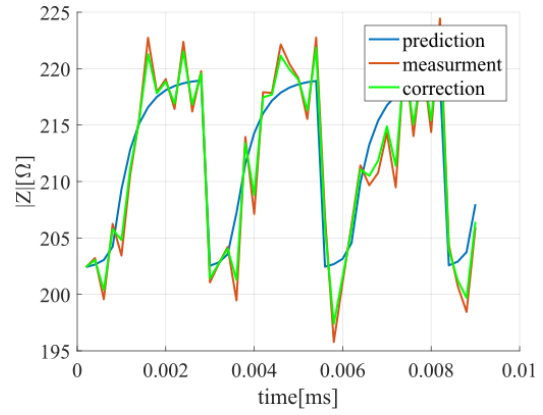


Fig. 5. Simulation results of the Kalman filter for $R = 4$, $Q = 10$

measurements.

5. Real Time Kalman Filter for Impedance Measurements Identification

In this section, the Kalman filter is described by presenting the main equations and parameters. It will be used for filtering the impedance's evolution in function of the position. All developments have been done by considering a constant speed operation. For the moment, we are considering this speed as being known a priori (11).

5.1 Kalman Filter Theory The discrete Kalman filter algorithm is described in (12). Time update equations are:

$$\hat{X}_k^- = A \hat{X}_{k-1} + B u_{k-1}, \quad \dots \quad (2)$$

$$P_k^- = A P_{k-1} A^T + Q, \quad \dots \quad (3)$$

measurement update equations are:

$$K_k = \frac{P_k^- H^T}{H P_k^- H^T + R}, \quad \dots \quad (4)$$

$$P_k = (1 - K_k H) P_k^-, \quad \dots \quad (5)$$

$$\hat{X}_k = \hat{X}_k^- + K_k (X_{\text{meas},k} - H \hat{X}_k^-), \quad \dots \quad (6)$$

where X_k is the variable state, the matrix A relates the state X_k to the previous one X_{k-1} . The matrix B links input u to the state X_k . X_{meas} is the measured state and H the measurement transfer matrix. \hat{X}_k^- is the a priori state estimation and \hat{X}_k the a posteriori state estimation. P_k^- and P_k are respectively the a priori and the a posteriori state estimate error covariance. K_k the Kalman gain. Q and R are respectively the process noise covariance and the measurement noise covariance.

5.2 Simulation Results For a displacement of the wagon with a constant speed of 0.6 m/s, Fig. 5 shows the filter results for $R = 4$, $Q = 10$, where we can see that the filter is not really effective. Figure 6 shows the filter results for $R = 5.6$ and $Q = 0.1$ where a good agreement between estimated, measurements, and corrected impedance could be verified. In red the noisy impedance variation, in blue the model impedance variation, in green the filtered impedance.

One can observe that impedance obtained without moving the wagon (Fig. 4) is smoother than the impedance shown in Fig. 5 because of the noise provoked by speed.

In this first Kalman filter, the value of the speed is needed in order to have a good estimation on the impedance level in

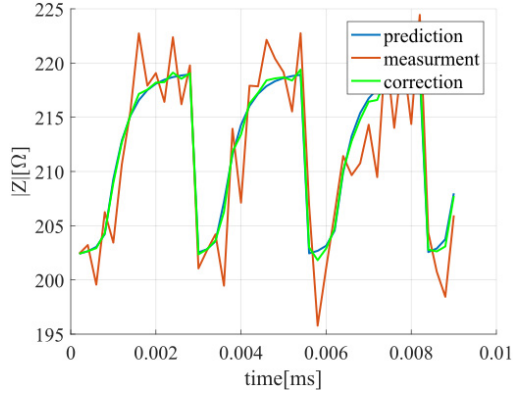


Fig. 6. Simulation results of the Kalman filter for $R = 5.6$, $Q = 0.1$

the filter algorithm, thus a second Kalman filter has been developed for the estimation of the speed based on impedance measurements.

6. Real Time Kalman Filter for Speed Identification

Since our model gives the impedance level with respect to the position, the a priori value of the impedance is highly linked to a good a priori value of the position. Thus, a good estimation of the speed is needed.

6.1 Adapted Kalman Filter Finding the speed using a Kalman filter consists in tracking a random constant value. Therefore the filter equations (2), (3), (4), (5), and (6) can be adapted as follows:

$$\hat{V}_k^- = \hat{V}_{k-1}, \dots \dots \dots (7)$$

$$P_k^- = P_{k-1} + Q, \dots \dots \dots (8)$$

Measurement update equations:

$$K_k = \frac{P_k^-}{P_k^- + R}, \dots \dots \dots (9)$$

$$P_k = (1 - K_k) P_k^-, \dots \dots \dots (10)$$

$$\hat{V}_k = \hat{V}_k^- + K_k (V_{\text{meas},k} - \hat{V}_k^-), \dots \dots \dots (11)$$

where \hat{V}_k^- is the a priori speed estimation and \hat{V}_k the a posteriori estimation. V_{meas} is the measured speed.

6.2 Speed Determination Algorithm The measured speed is obtained in two steps: at first the period of the measured impedance is determined using normalized autocorrelation function which is an accurate method for determining the period of a noisy signal, as follows:

$$r_k = \frac{1}{E_k} \left(\frac{1}{N} \sum_{i=k-N}^{i=k} z_{\text{meas}}(i) z_{\text{meas}}(i+n) \right), \dots \dots \dots (12)$$

$n = 0, 1, 2, \dots, N-1$

where r_k is the autocorrelation vector at step k , E_k the signal energy, N the number of samples, and z_{meas} the vector of N measured values. The main motivation of using time domain method also known as autocorrelation based method for determining the period is that the observation of z_{meas} is periodic. Therefore, the vector r_k will also show a period t_k . The peaks of r_k occurs at values of discrete time equal to t_k

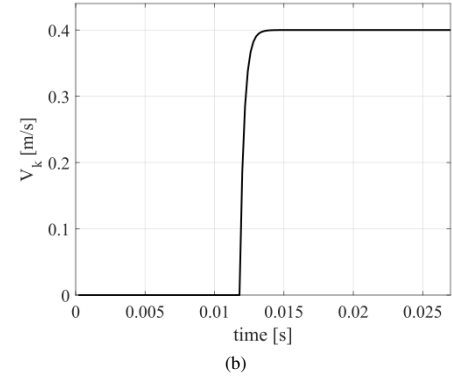
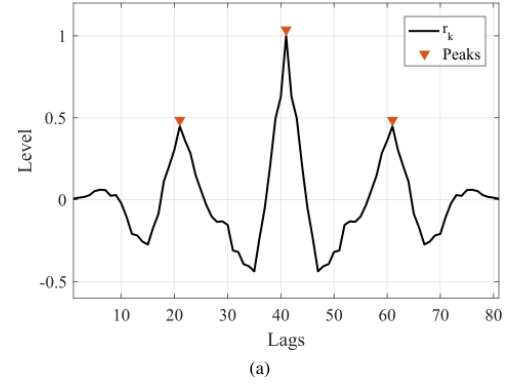


Fig. 7. (a) Example of vector r_k with large peaks (b) Speed learning curve for a settled speed of 0.4 m/s

and its multiples as shown in Fig. 7.

This period calculation need to be continuous consequently we have used a sliding window of N samples. The autocorrelation curves gives us peaks where the samples are similar, and then the lag of the largest peaks is taken for calculating the estimated period at each step, as follows:

$$t_k = \Delta \text{Lag} \times T_s, \dots \dots \dots (13)$$

where t_k is the period at the instant k in discrete time, ΔLag the largest peaks lag difference, and T_s the sampling period of the system.

By knowing the distance P_c (the gauge) between two keys, the speed is then calculated as follows:

$$V_{\text{meas},k} = \frac{P_c}{t_k}, \dots \dots \dots (14)$$

6.3 Results Figure 8 shows the speed learning curve for a settled constant speed of 0.4 m/s where a good learning process could be verified. This estimation has been obtained by using a ΔLag calculated with a fixed level of 0.35. To a further discussion on the influence of this level on estimations see section 8.2

7. Simultaneous Kalman Filters for Sensorless Control

The use of two Kalman filters for both state variables and parameter estimation was firstly proposed in (13) and (14) the use of Kalman filtering for parameter estimation has led to a sensorless control of a BLDC motor. In this section the use of two parallel Kalman filters is described.

7.1 Parallel Kalman Filter Algorithm The basic operation of the parallel filters is drawn in Fig. 8, where $X^$

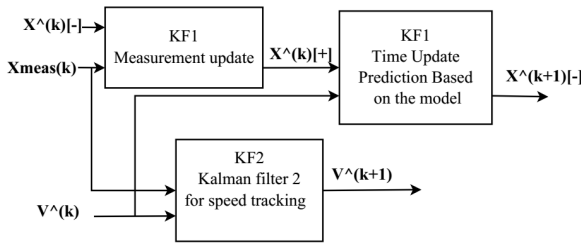


Fig. 8. Functioning scheme of the two parallel Kalman filters

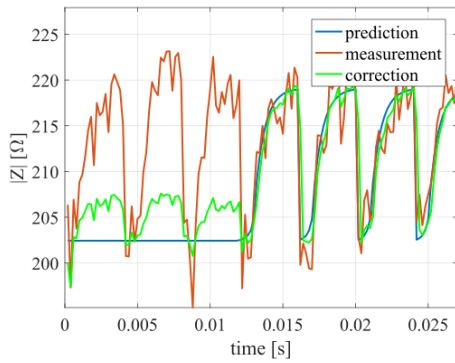


Fig. 9. Noisy impedance filtering for $V = 0.4$ m/s

stands for the estimated state \hat{X}_k , \hat{V}_k for the estimated speed \hat{V}_k , k is the instant in the discrete time, $[-]$ is for a priori variables and $[+]$ is for a posteriori variables.

The designed system works in two phases: at first the initialisation process where the estimated position and the estimated speed are null, in KF1 the calculated \hat{X}_k takes into account only the measured values $X_{\text{meas},k}$, since no prediction on the state \hat{X}_k^- can be done without a good estimation of the speed; and in KF2 the system accumulates the measured values of impedance while the wagon is in displacement, till the number of samples required for calculating the first value of the speed is reached. Since the assumption of a constant speed has been made, the system will consider the elapsed time and the first value of the estimated speed to produce the first value of the estimated position. Secondly, the system starts to produce the corrected values of the measured impedance while estimating its speed at the same time.

7.2 Results For a settled value of the speed 0.4 m/s the system response is shown in Fig. 9 where we can see that after the speed tracking process, both filters are launched and a good agreement between the measurements and the system correction could be verified.

For a settled speed of 0.8 m/s the system response is shown in Fig. 10 and Fig. 11, where we can also see a good agreement between the measured impedance and the filtered impedances.

Both results, displacement of 0.4 m/s and 0.8 m/s, shows that considering the wagon's speed and the response time (numerical implementation of the Kalman Filters), several keys are needed to estimate the speed. This is due to the learning process.

8. Optimizing Kalman Filter Parameters

In the previous section of the paper the Kalman filters variables Q and R were chosen by fine-manually tune in other

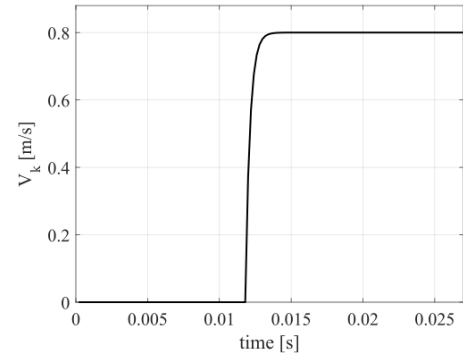


Fig. 10. Speed tracking curve for a settled speed of 0.8 m/s

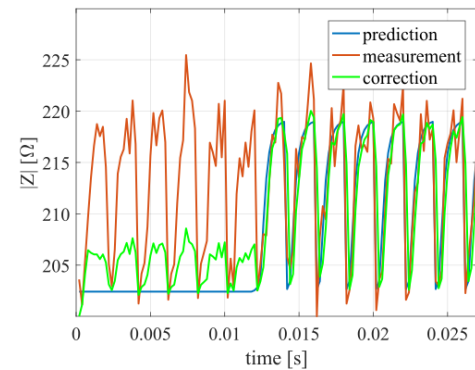


Fig. 11. Noisy impedance filtering for $V = 0.8$ m/s

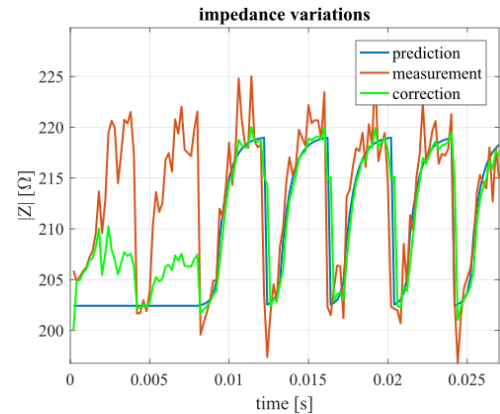


Fig. 12. New noisy impedance filtering for $V = 0.4$ m/s

to achieve a good agreement between the measurements and the model. Therefore, it is important to know the distribution of the disturbances and measurement noises. In this section we will describe a simple approach to have a good estimation of the values of those two parameters.

8.1 Offline Model Simulation for Process Noise Covariance Determination Defining the process error covariance Q as the error covariance between our model and real measurements, this value can be computed offline as follows:

$$Q = \frac{1}{N} \sum_{k=1}^N (e_1(k) - \bar{e}_1)^2, \dots \quad (15)$$

with e_1 error vector between the real measurements and the model, \bar{e}_1 the mean value of the error and N the number of samples taken into account. The error vector is obtained as

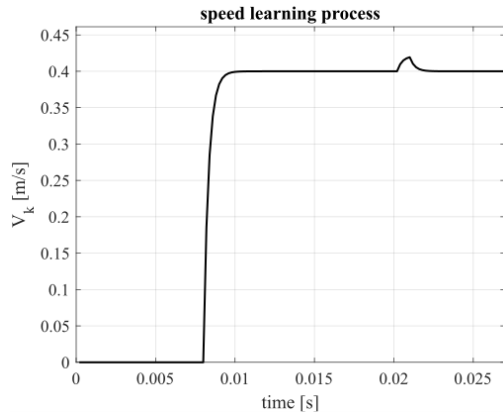


Fig. 13. New speed tracking curve for a settled speed of 0.4 m/s

follows

$$e_1 = |z_{model} - z_{real}|, \dots \dots \dots (16)$$

with z_{model} the impedance variations given by the model in function of the position, z_{real} the level of impedance given by the impedance measurement in function of the position (considered as real values). Thus, the obtained value of Q is 4.0314. Therefore, as our model definition does not vary within the time, the value of Q can be left constant at the obtained value.

8.2 Real Time Parameters Calculation Since the disturbances and noises in measurement cannot be defined correctly, the value of R is calculated iteratively using the past knowledge of the impedance measurements and the model prediction. The value of R is obtained as follows:

$$R = \frac{1}{N} \sum_{k=1}^N (e_2(k) - \bar{e}_2)^2, \dots \dots \dots (17)$$

where e_2 is the error between the measurements and the model, \bar{e}_2 the mean value of the error, N the accumulated number of samples or the sliding window length. The vector \bar{e}_2 is obtained as follows:

$$e_2 = |z_{meas} - z_{model}|, \dots \dots \dots (18)$$

here z_{model} is the same as the predicted value of impedance. For a settled value of speed $V = 0.4$ m/s and for $Q = 4.0314$, Fig. 13 shows the new response curves of the impedance filtration, Fig. 14 the new speed learning process.

The time response of the speed tracking in this section has been improved. The first estimation of the speed is obtained after the first period of Keys. Since the calculation of the speed rely on the measurement of the first period of Keys, the autocorrelation vector may be affected by noise and disturbances because the of the limited number of measurement taken into account; that can produce some errors in the estimation of le lags of largest peaks and thus the speed estimation. Therefore, those errors doesn't have a huge effect on the identification since we can still count the same number of keys as shown in Fig. 15 and Fig. 16.

The temporal evolution of the Kalman gain and the variation of the measurement noise covariance are shown in Fig. 17 and Fig. 18, respectively.

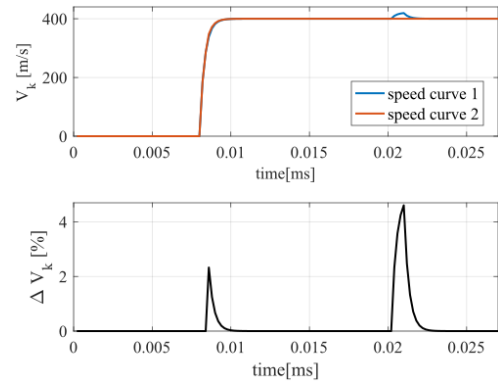


Fig. 14. Comparison between two speed calculation curves

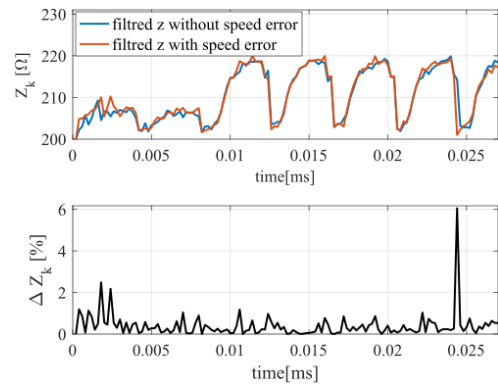


Fig. 15. Comparison between two filtered impedance

The Kalman gain K starts at a value of 1 because the system relies only on the measurement at this step, since there is no predicted data and no accurate value of the variable R. With the first measurements, values of variable R became available and the Kalman gain K start to be calculated properly till it converges towards a constant value. The estimation of the variable R starts to be accurate enough because of the recorded past values of measurements.

8.3 Comparison between the Previous Kalman Filter and the New Kalman Filter for the Speeds 0.4 m/s and 0.8 m/s The aim of this section is to compare performances of the standard method and the new one by observing the error on the filtered and ideal impedances. Fig. 19 and Fig. 20 show results for for settled speeds of 0.4 m/s and 0.8 m/s.

On these figures, we can see that on most of samples, the new Kalman filter (orange curve) has a smaller error compared to the previous Kalman system (blue line). By using the following definition of the total error:

$$error = \frac{1}{N} \sum_{k=1}^N abs(\Delta Z(k)), \dots \dots \dots (19)$$

we get, for a settled speed of 0.4 m/s, 2.29 and 1.92 before and after the optimization of parameters, respectively.

This error is calculated in respect to the maximum value to avoid increasing the error when the impedance is very small.

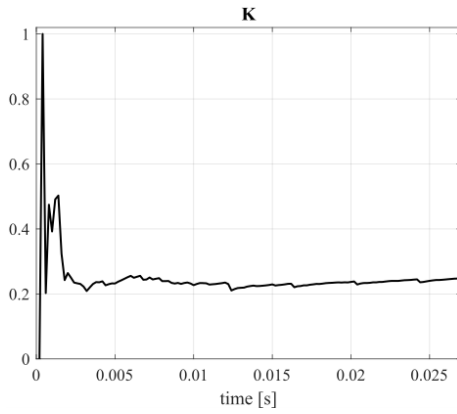


Fig. 17. Temporal evolution of parameter K for a settled speed of 0.4 m/s

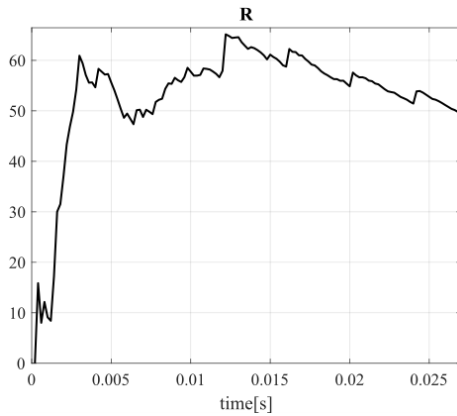


Fig. 18. Temporal evolution of parameter R for a settled speed of 0.4 m/s

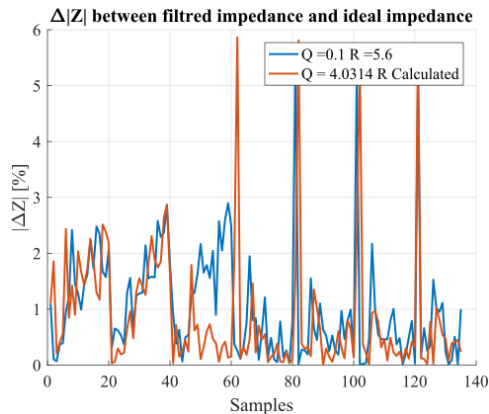


Fig. 19. Temporal evolution of parameter K for a settled speed of 0.4 m/s

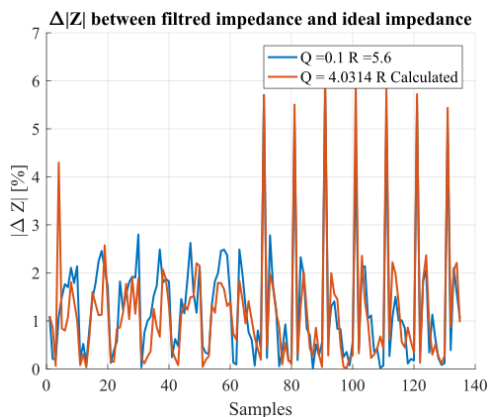


Fig. 20. Temporal evolution of parameter K for a settled speed of 0.8 m/s

9. Conclusion

This work shows a new method for position control of a textile machine Hybrid Linear Switched Reluctance Actuator by using only the actuator impedance as information. The originality of the presented method is to show an efficient way to implement a speed and impedance filters for a parallel real time operation applied to linear actuators. Furthermore, we were able to develop the entire process from modelling by parameter identification to how optimize parameters to minimize errors between the filtered impedance and the real one. For a settled speed of 0.4 m/s the total error have been decreased of 16%.

References

- (1) I. Boldea: "Classifications and Applications of LEMs", in Linear Electric Machines, Drives, and MAGLEVs Handbook, CRC Press (2013)
- (2) P. Liu, C. y Hung, C. s Chiu, and K. y Lian: "Sensorless linear induction motor speed tracking using fuzzy observers", JET Electr. Power Appl., Vol.5, No.4, pp.325–334 (2011)
- (3) J.I. Ha and S.K. Sul: "Sensorless field-orientation control of an induction machine by high-frequency signal injection", IEEE Trans. Ind. Appl., Vol.35, No.1, pp.45–51 (1999)
- (4) Z. Chen, M. Tomita, S. Doki, and S. Okuma: "An extended electromotive force model for sensorless control of interior permanent-magnet synchronous motors", IEEE Trans. Ind. Electron., Vol.50, No.2, pp.288–295 (2003)
- (5) J. Maridor, et al.: "Kalman filter to measure position and speed of a linear actuator", IEEE International Electric Machines & Drives Conference (IEMDC) (2011)
- (6) D. Vinh Do, et al.: "Impedance observer for a Li-ion battery using Kalman filter", in IEEE Transactions on Vehicular Technology, Vol.58, pp.3930–3937 (2009)
- (7) M. Vaukonen, P.A. Karjalainen, and J.P. Kaipio: "A Kalman filter approach to track fast impedance changes in electrical impedance tomography", in IEEE Transactions on Biomedical Engineering, Vol.45, pp.486–493 (1998)
- (8) W.-C. Gan, N.C. Cheung, and L. Qiu: "Position control of linear switched reluctance motors for high-precision applications", IEEE Trans. Ind. Appl., Vol.39, No.5, pp.1350–1362 (2003)
- (9) W. Helbach, P. Marcinowski, and G. Trenkler: "High-Precision Automatic Digital AC Bridge", IEEE Trans. Instrum. Meas., Vol.32, No.1, pp.159–162 (1983)
- (10) M.R.A. Calado, A.E. Santo, S.J.P.S. Mariano, and C.M.P. Cabrita: "Characterization of a new linear switched reluctance actuator", in 2009 International Conference on Power Engineering, Energy and Electrical Drives, pp.315–320 (2009)
- (11) F.T. Simo, D.M. Araujo, and Y. Perriard: "Sensorless Method with Parameter Identification Applied to a Bistable Fast Linear Switched Reluctance Actuator for Textile Machine", the 11th International Symposium on Linear Drives for Industry Applications (2017)
- (12) G. Welch and G. Bishop: "An introduction to the kalman filter", University of North Carolina at Chapel Hill (2006)
- (13) L. Nelson and E. Stear: "The simultaneous on-line estimation of parameters and states in linear systems", IEEE Transactions on Automatic Control, Vol.21, No.1
- (14) O. Scaglione, et al.: "On-line Parameter Estimation for Improved Sensorless Control of Synchronous Motors", 2012 IEEE International Electric Machines Conference (ICEM) (2012)



Douglas Martins Araujo (Non-member) received the electrical engineering and the Msc. degrees from the Federal University of Santa Catarina, Brazil, and the National Polytechnic Institute of Toulouse, France, in 2011. He received the Ph.D. degree from the National Polytechnic Institute of Grenoble, France, in 2015. After a period as a researcher fellow in the French Alternative Energies and Atomic Energy Commission, he joined the Swiss Federal Institute of Technology (EPFL), in Switzerland. His research interests are in the field of electromechanical devices, numerical methods and nondestructive testing.



Faguy Tamwo Simo (Non-member) received the Master degree in Electrical Engineering from the National Advanced School of Engineering Yaoundé (ENSPY) in 2016. He has worked with the research team of Integrated Actuators Laboratory (EPFL-LAI) on the study of an industrial knitting machine actuator. His scientific interests are Control-Command of Electrical systems and their applications.



Yves Perriard (Non-member) received the M.Sc. degree in micro-engineering and the Ph.D. degree from the Swiss Federal Institute of Technology (EPFL), Lausanne, in 1989 and 1992, respectively. He was the cofounder and Chief Executive Officer of Micro-Beam SA which is involved in high-precision electric drives. He is with EPFL, Neuchâtel, Switzerland, where he was a Senior Lecturer in 1998, has been a Professor since 2003, and is currently the Director of the Laboratory of Integrated Actuators. From 2009 to 2013, he has been the Vice-Director of the Microengineering Institute, Neuchâtel, Switzerland. His research interests are in the field of new actuator design and associated electronic devices. Dr. Perriard is a Vice-President of the Executive Council of the European Power Electronics Association, Brussels, Belgium.